

Photoexcited states of the harmonic honeycomb iridate γ -Li₂IrO₃

J. P. Hinton,^{1,2} S. Patankar,^{1,2} E. Thewalt,^{1,2} J. D. Koralek,¹ A. Ruiz,^{1,2} G. Lopez,^{1,2}
N. Breznay,^{1,2} I. Kimchi,² A. Vishwanath,^{1,2} J. Analytis,^{1,2} and J. Orenstein^{1,2}

¹Materials Science Division, Lawrence Berkeley National Laboratory, Berkeley, California 94720, USA

²Department of Physics, University of California, Berkeley, California 94720, USA

(Dated: December 7, 2024)

We report results of equilibrium and nonequilibrium optical measurements of the "harmonic" honeycomb γ -Li₂IrO₃, as well as the layered honeycomb iridate Na₂IrO₃, as a function of time, temperature and polarization. The photo-modulated reflectivity $\Delta R(t, T)$ is strikingly similar in the two systems in the limiting regimes of high (~ 300 K) and low (~ 5 K) temperature, exhibiting a short-lived excited state at high T that is accompanied by a much longer lived state at low T . Despite the similarity at the two limits of T , the evolution of the $\Delta R(t, T)$ between these regimes is markedly different; a smooth and isotropic T dependence in Na₂IrO₃, contrasting with abrupt changes in amplitude and anisotropy coinciding with the onset of magnetic correlations in γ -Li₂IrO₃.

Transition metal oxides (TMO) host complex phases resulting from interactions with a hierarchy of energy scales. In $3d$ and $4d$ TMOs, competition between kinetic energy, quantified by the parameter, t , and Coulomb repulsion, parameterized by U , are the major factors determining the nature of lowest energy phases. However, in $5d$ systems the spin-orbit (SO) interaction, which plays a subsidiary role in the lighter TMs, becomes an equal partner in shaping the nature of the electronic states.

The iridate family of TMOs are a particularly striking example of interplay between SO and U interactions. It is proposed that the strong SO interaction reorganizes the crystal field states of the $5d$ orbitals into a J -multiplet structure, where J is the combined spin and orbital angular momentum. The relatively weak U is then sufficient to produce localization in the singly occupied $J = 1/2$ doublet, giving rise to a novel Mott insulator in which the local moments have both spin and orbital character [1, 2]. Despite its appeal, this physical picture remains controversial, in as much as quantum chemical considerations suggest that SO, U , t , and crystal field interactions are of comparable magnitude, such that neither a local J -multiplet or delocalized orbital picture is entirely appropriate [3–9].

In addition to the questions concerning the origin of the insulating ground state, there is considerable interest in the magnetic correlations in iridates. In compounds of the form A₂IrO₃, where A is Na or Li, the combination of strong SO coupling and edge sharing IrO₆ octahedra is thought to give rise to anisotropic Kitaev magnetic exchange [10, 11]. Na₂IrO₃ (NIO), which possesses a layered honeycomb structure, was the first iridate to be scrutinized in the search for a realization of the Kitaev spin liquid. However, neutron and X-ray diffraction studies revealed a rather simple form of magnetic order: a coplanar antiferromagnet with a zigzag structure [13–15]. Given this conventional form of magnetic order, it is difficult to argue that Kitaev interactions dominate the other symmetry allowed spin couplings in this system [7, 16, 17].

Recently, two polytypes of Li₂IrO₃, β [18] and γ [19], have been synthesized with structures that were previously unknown. Each of these has the same basic building block

of three-fold coordinated Ir ions as the layered honeycomb structure. However, in both new polytypes the plane formed by the triad of Ir links rotates to create three dimensional rather than layered structures. In contrast to the comparatively conventional magnetic structure in NIO, these harmonic honeycomb iridates host pairs of incommensurate, non-coplanar, and counter-propagating spin spirals [20]. Comparison with the ground state of model spin Hamiltonians suggests that Kitaev interactions must dominate Heisenberg terms in order to produce the complex spin spirals that are observed [21–24].

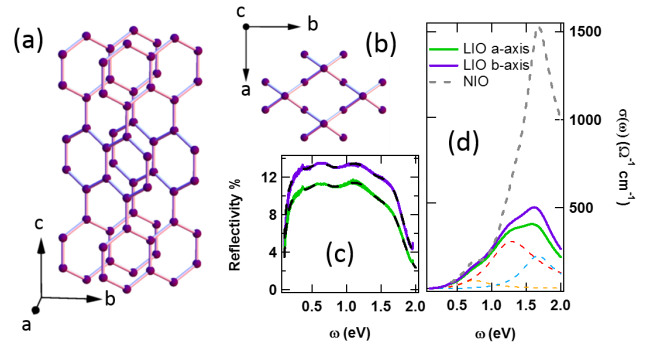


FIG. 1. (a) Three dimensional view of the crystal structure of LIO, with only the iridium atoms shown for simplicity. (b) The same structure as viewed along the crystallographic c -axis. (c) The optical reflectivity along the a (green) and b (purple) axes in LIO. Lorentz oscillator fits shown in black dash. (d) Optical conductivity of LIO and NIO. The green and purple curves correspond to the a and b -axis optical conductivity, respectively, in LIO, and the NIO data from reference [9] is shown by the gray dash. The thin colored dashed lines show the oscillators used to fit the reflectance data from (c).

The detailed knowledge of the magnetic order of the new iridate compounds is in sharp contrast with our understanding of their electronic structure, both from an experimental and theoretical point of view. In the case of the layered honeycomb iridates, the results of RIXS, PES, and optical spectroscopy, considered together with T -dependence of the resistivity, point to an insulating state with a bandgap on the order of 0.5 eV [4, 9, 12, 25]. Far less is known about γ -Li₂IrO₃

(LIO) because of its recent discovery, as well as the relatively small (100 μm) dimensions of crystals synthesized to date. In this Letter we report measurements of electronic properties using two optical methods. We have used Fourier transform infrared microscopy to perform broadband polarized measurements of the infrared reflectivity LIO single crystals, from which we extract the two in-plane components of the optical conductivity tensor in the range from 0.2 to 2.0 eV. In addition, in order to reveal small changes in the reflectivity with temperature that may be associated with spin order, we have performed transient optical reflectivity measurements using 100 fs pulses of 1.5 eV photons. The comparison of the results on NIO and LIO reveal surprising differences in the optical properties of these two compounds, with implications for the nature of the coupling between magnetic order and electronic states.

Figs. 1a and 1b illustrate the atomic structure of LIO. Fig. 1a provides a 3D perspective on the overall crystal structure, showing only the Ir atoms for clarity. The structure is seen to consist two sets of chains of hexagons, oriented in the directions $\mathbf{a}\pm\mathbf{b}$. A hexagon that lies in one set of such chains is connected to its nearest neighbor chain through an Ir-Ir link oriented in the c -direction. The surface of the crystals suitable for optical microscopy is the plane perpendicular to \mathbf{c} , as shown in Fig. 1b.

The optical spectra in Fig. 1c show that the reflectivity, R , is quite low over the entire spectral range and furthermore that the difference in R for light polarized along the a and b axes is rather small. The fits to the reflectivity were obtained by modeling the optical conductivity as a sum of contributions from four Lorentz oscillators at 0.4, 0.7, 1.3, and 1.7 eV. Excellent fits were obtained for the two principal axes using the same resonance frequency and damping but slightly different oscillator strengths. The optical conductivity thus obtained (shown as solid lines) is quite similar to that found at low energy in NIO (< 1 eV), but is substantially smaller at higher energy. Calculations of optical conductivity have been performed within density functional theory (including both SO and U couplings) for the layered honeycomb polytype of Li_2IrO_3 and Na_2IrO_3 [26]. The spectra that emerge from this theory are quite similar for these two compounds, suggesting that the large difference we observe is a consequence of the inherently 3D structure of $\gamma\text{-Li}_2\text{IrO}_3$, rather than the replacement of Na by Li.

The T dependence of the reflectivity spectra is quite weak with both NIO and LIO, and does not show clear features at the temperature of magnetic phase transitions. However, hidden structure in $R(T)$ can be enhanced using modulation spectroscopy, for example as in this work, by time-resolving the change in $R(T)$ induced by photoexcitation with a sub-picosecond light pulse. In materials that undergo phase transitions, the photoinjected entropy and energy generally lead to a weakening of the equilibrium order parameter [27, 28]. Typically, there is a bottleneck for the flow of energy/entropy in time from the photoexcited electrons to the collective modes of the order parameter. Largely because of this bottleneck,

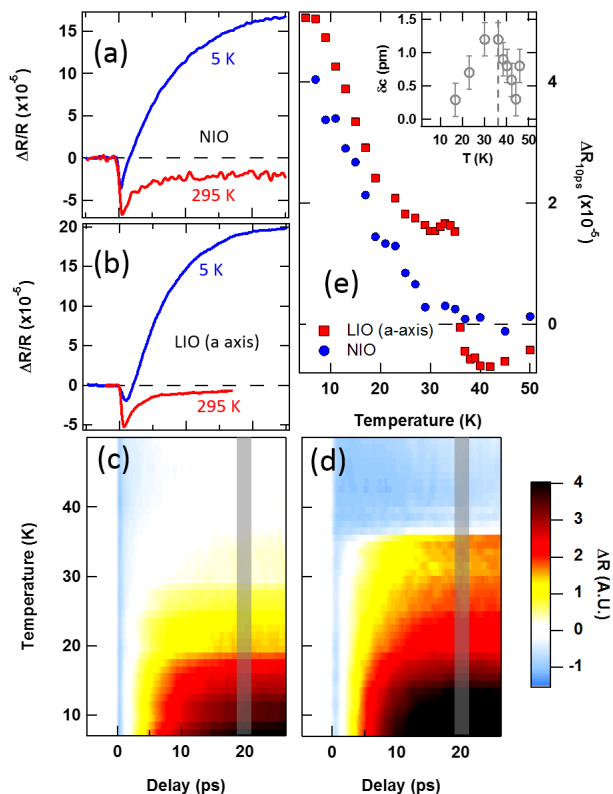


FIG. 2. Pump-probe reflectivity at room temperature (red) and 5 K (blue) is shown for NIO in (a) and along the LIO a-axis in (b). (c) and (d) show $\Delta R(t, T)$ as a false color image for NIO and a-axis LIO, respectively. (e) $\Delta R(t = 20 \text{ ps}, T)$ from (c) and (d), plotted as a function of temperature. The T dependence seen in the two compounds is quite similar below 30 K, but note the abrupt jump in the LIO response near T_c , which is entirely absent in NIO. The inset shows temperature dependence of the c -axis lattice constant registered to 1779.5 pm [19].

the onset of magnetic order can be seen clearly in the amplitude and time-dependence of the nonequilibrium optical properties [29–31].

The temperature and delay time dependence of the photoinduced change in reflectivity, $\Delta R(t, T)$, for LIO and NIO are compared in Fig. 2. Figs. 2a and 2b show $\Delta R(t)$ of the two compounds at room temperature and at 5 K. The magnitude, sign, and time dependence of the response in the two materials are strikingly similar in these two limiting regimes of T . At room temperature $\Delta R(t)$ is negative with an abrupt onset of less than 1 ps duration. From optical and RIXS spectroscopy of the iridates, as well as theoretical calculations, it is clear that the pulse of 1.5 eV photons excites electrons within the Ir t_{2g} manifold. The initial rapid decay of $\Delta R(t)$ likely reflects the cooling of electrons and holes as they reach quasi-thermal equilibrium with the lattice. The ultimate return to equilibrium of the coupled electron-phonon system then takes place on the nanosecond timescale. At low T , the negative reflectivity transient is accompanied by a positive component of $\Delta R(t)$

that rises on much slower, ~ 10 ps, time scale. As discussed above, this slow onset indicates coupling to collective modes of an ordered system.

Although $\Delta R(t)$ is similar in LIO and NIO at both low and high T , the pathway to these regimes is quite different, particularly in the range of T where magnetic order appears. $\Delta R(t, T)$ for NIO and LIO is shown as a false color image in Figs. 2c and 2d, respectively. In NIO the positive signal emerges gradually upon cooling below ~ 40 K whereas in LIO it appears abruptly at approximately the magnetic transition temperature, T_c , of 36 K. This contrasting behavior is shown clearly in Fig. 2e, where $\Delta R(T)$ for the two compounds at $t = 20$ ps is compared.

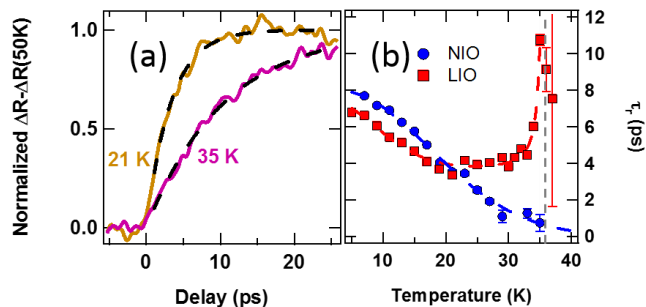


FIG. 3. (a) The positive component of $\Delta R(t)$ in LIO at 21 K and 35 K, isolated by subtracting $\Delta R(t)$ at 50 K, and normalized. The exponential fit is shown in black dash. (b) The temperature dependence of the exponential risetime obtained from the fits in (a). Note that τ_r diverges at T_c in LIO, while there is no feature at the magnetic transition temperature of 15 K in NIO.

The sudden onset of the positive component of ΔR at T_c in LIO suggests that it is closely related to magnetic order. Further indication of its magnetic origin is the T dependence of its rise time, τ_r . To determine τ_r the positive signal was isolated by subtracting $\Delta R(t, T = 50 \text{ K})$ from the curves at lower T , as shown in Fig. 3a. The resulting single component signals can be accurately fit with an exponential rise of the form, $1 - e^{-t/\tau_r}$. In Figure 3b we plot $\tau_r(T)$ thus obtained for both compounds. The contrasting behavior of LIO and NIO seen in the amplitude of ΔR appears clearly in the temperature dependence of τ_r as well. Whereas in NIO the rise time increases smoothly with decreasing T , in LIO it diverges at T_c . Divergence of τ_r at T_c has been observed in many systems undergoing magnetic phase transitions [29–31], and is considered to be a signature of photoinduced demagnetization. The slow rise time throughout the ordered state is understood on a phenomenological level to be a consequence of weak coupling between electron and spin sub-systems. The divergence of τ_r near T_c emerges naturally in such two-temperature models as a result of the vanishing of the mean exchange field at the transition [31, 32].

The step-like change in ΔR at the magnetic transition is consistent with the combined effect of photoinduced demagnetization and magnetoelastic coupling. The inset to Fig. 2e

shows the discontinuous change in slope of the c -axis lattice constant (a_c) that occurs at T_c , indicating a substantial magnetoelastic coupling, $\alpha \equiv \partial a_c / \partial M$, where M is the magnetic order parameter [19]. Since, in general, R couples linearly to the lattice constant, we expect a change in R with fluence Φ given by $\partial R / \partial \Phi = \alpha (\partial R / \partial a_c) (\partial M / \partial \Phi)$. The observation that the time required for the jump in ΔR at T_c to appear is at least 10 ps and diverges at T_c indicates that it arises from photo-demagnetization rather than a photoinduced increase in lattice temperature.

For magnetic insulators such as LIO and NIO, it is reasonable to imagine that photo-demagnetization occurs via local distortion of magnetic order in the neighborhood of each of the non-equilibrium quasiparticles. A specific proposal, put forward in the interpretation of transient reflectivity measurements on NIO [33], is that ΔR corresponds to a nonequilibrium population of unoccupied sites (holons) and doubly occupied sites (doublons). The positive reflectivity transient at low temperature is then attributed to the binding of these excitations due to the energy cost of deforming the “zigzag” magnetic structure. However, we observe that the low temperature reflectivity dynamics are essentially identical in NIO and LIO. This indicates that the properties of quasiparticles in these compounds are shaped by common features in their local electronic structure, independent of the long-range magnetic order.

The importance of local structure is also suggested by the dependence of $\Delta R(t, T)$ on the direction of the electric field, \mathbf{E} , in the plane of the reflecting surface. While in NIO the response is isotropic, a strong anisotropy appears in LIO with decreasing T . Fig. 4a compares $\Delta R_a(t, T)$ and $\Delta R_b(t, T)$, the change in reflectivity with probe \mathbf{E} parallel to the a and b axes, respectively, for a series of temperatures that span T_c . The a -axis data for each temperature is shown in light green, with the b -axis data in purple. Within experimental error, the response is isotropic for $T \geq 65$ K. Below this temperature, but still well above T_c , the response in the two directions becomes distinguishable.

To make more clear how the anisotropy develops, at each T we plot (as a gray dashed line) the isotropic signal observed at $T = 70$ K. The blue shading indicates a positive difference relative to the response at 70 K, whereas red shading indicates a negative difference. Figs. 4b and 4c encapsulate the onset of anisotropy in $\Delta R(t, T)$ in LIO by considering $\langle \Delta R(t, T) \rangle_t$, the change in reflectivity averaged over the time-delay interval from 0 to 50 ps. $\langle \Delta R(t, T) \rangle_t$ is plotted for each of the two directions of the probe \mathbf{E} in Fig. 4b and the difference between them, $\langle \Delta R_a(t, T) \rangle_t - \langle \Delta R_b(t, T) \rangle_t$ is shown in Fig. 4c.

Fig. 4 illustrates the complexity of the temperature dependent optical anisotropy. Upon cooling, $\Delta R_b(t, T)$ varies from the isotropic high- T signal starting at 65 K, whereas $\Delta R_a(t, T)$ is roughly T independent. As the sample temperature reaches T_c , the anisotropy becomes dominated by the abrupt onset of a positive signal in the a -axis channel. A similar positive component is apparent in the b -axis data, but its onset is much more gradual.

The observation that $\Delta R_b(t, T)$ is special for $T > T_c$ is consistent with a unique structural feature of the LIO harmonic honeycomb. As depicted in Fig. 4d, there are two c-oriented links in LIO: one that bridges two chains of hexagons and another that forms a bond in each Ir hexagon. The popout in Fig. 4d shows an expanded view of an Ir triad that contains a bridging c-axis link. The hopping between linked Ir atoms is mediated by the two nearest neighbor O atoms, which all together form a coplanar Ir-O₂-Ir unit. In the γ -Li₂IrO₃ structure, as opposed to the layered honeycomb, the normal to this plane is parallel to a principal axis, namely b. By contrast, the IrO₂ planes in the layered honeycomb structure are neither parallel nor perpendicular to the layer plane.

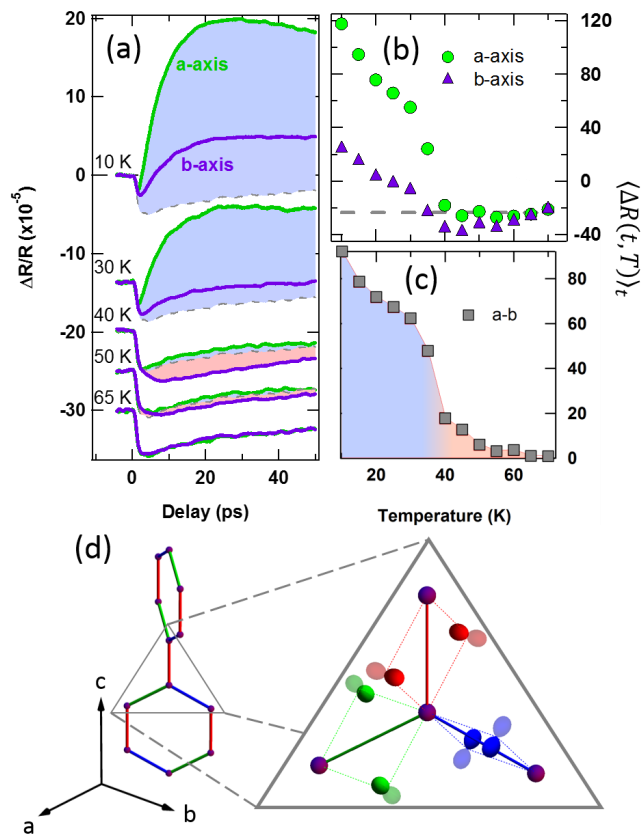


FIG. 4. (a) The pump-probe response in LIO with probe-polarization along the a and b axes is shown for a series of temperatures spanning T_c . The a-axis data for each temperature is shown in green, with the b-axis data in purple. The dashed gray lines show the 70 K data as reference, with the blue shading indicating a positive difference from the 70 K signal and red shading indicating a negative difference. (b) The integrated area under the a and b-axis curves from (a). (c) The difference in integrated area between the a and b axes. (d) A schematic illustration of the arrangement of two iridium hexagons in LIO that belong to nearest neighbor chains. The x, y, and z Kitaev bonds are shown in blue, green, and red, respectively, with the principal crystallographic axes in black. The triangular popout shows the oxygen 2p orbitals involved in hopping between the neighboring iridium atoms.

The fact that, in LIO, ΔR_b deviates from the high- T isotropic signal well above T_c suggests that magnetic correlations develop in the normal state initially on the b-axis oriented Ir-O₂-Ir planes. This observation is consistent with the magnetic susceptibility, χ , of LIO, where it is found that χ_b grows much more rapidly than χ_a and χ_c as the temperature is lowered towards T_c [19]. The nearly divergent χ_b implies correlations of moments on the c-oriented Ir₂ links that favor ferromagnetic alignment in the b-axis direction. This is precisely the correlation that is expected to develop from the Kitaev interaction. When this coupling is sufficiently dominant, the ground state is expected to be a spin liquid, rather than a magnetically ordered state [22].

The transition to magnetic order in LIO at 35 K indicates that subdominant magnetic interactions destabilize the spin liquid state. Theoretical analysis indicates that complex pattern of counterpropagating, noncoplanar spirals that is seen by X-ray diffraction is a consequence of subdominant Ising terms, such as $I_c S_1^c S_2^c$ in the case of the c-oriented links, together with the Kitaev couplings of the form $KS_1^y S_2^y$, where $\gamma = x, y, \text{ or } z$ as in Fig. 4a. The abrupt appearance of a positive component in both ΔR_a and ΔR_b at T_c is consistent with the idea that the spin order that onsets at T_c is distinct from the Kitaev-like spin alignment that appears in the normal state.

In summary, the optical properties of the NIO and LIO present an intriguing set of similarities and differences. The equilibrium optical conductivity of the two materials is virtually the same near the threshold for optical absorption, indicating the lowest energy electronic excitations are closely related. However the optical conductivity becomes quite different above 1 eV. The photoinduced reflectivity also manifests correspondences and contrasts. At the high and low limits of our range of temperatures, 290 K and 5 K respectively, the amplitude, sign, and time dependence of ΔR are virtually the same for the two compounds. However, the dynamics are strikingly different near the onset of magnetic ordering. In LIO, ΔR onsets discontinuously with the appearance of magnetic order, with a divergent rise time, while in NIO, ΔR develops smoothly without a divergent timescale. The nearly identical dynamics observed in the two compounds at low T , despite their sharp differences in long-range magnetic order, suggest that the excitations derive their metastability from local physics of the edge-sharing Ir-O octahedral structure that is common to both systems. Whether these excitations are topologically trivial, for example spin polarons, or more exotic topologically protected quasiparticles, remains a subject for future research into these complex materials.

We would like to thank T. Smidt, J. Neaton, and R. Valenti for illuminating discussion, as well as H. Bechtel and M. Martin for support at the Advanced Light Source (ALS) beamline 1.4.3 and 1.4.4. This work was supported by the Director, Office of Science, Office of Basic Energy Sciences, Materials Sciences and Engineering Division, of the U.S. Department of Energy under Contract No. DE-AC02-05CH11231.

-
- [1] B. J. Kim *et al.*, Phys. Rev. Lett. **101**, 076402 (2008).
- [2] B. J. Kim *et al.*, Science **323**, 345 (1961).
- [3] R. Arita, J. Kunes, A. V. Kozhevnikov, A. G. Eguiluz, and M. Imada, Phys. Rev. Lett. **108**, 086403 (2012).
- [4] R. Comin *et al.*, Phys. Rev. Lett. **109**, 266406 (2012).
- [5] D. Haskel *et al.*, Phys. Rev. Lett. **109**, 027204 (2012).
- [6] D. Hsieh, F. Mahmood, D. H. Torchinsky, G. Cao, and N. Gedik, Phys. Rev. B **86**, 035128 (2012).
- [7] I. I. Mazin, H. O. Jeschke, K. Foyevtsova, R. Valenti, and D. I. Khomskii, Phys. Rev. Lett. **109**, 197201 (2012).
- [8] I. I. Mazin *et al.*, Phys. Rev. B **88**, 035115 (2013).
- [9] C. H. Sohn *et al.*, Phys. Rev. B **88**, 085125 (2013).
- [10] J. Chaloupka, G. Jackeli, and G. Khaliullin, Phys. Rev. Lett. **105**, 027204 (2010).
- [11] Y. Singh *et al.*, Phys. Rev. Lett. **108**, 127203 (2012).
- [12] H. Gretarsson *et al.*, Phys. Rev. Lett. **110**, 076402 (2013).
- [13] X. Liu *et al.*, Phys. Rev. B **83**, 220403(R) (2011).
- [14] S. K. Choi *et al.*, Phys. Rev. Lett. **108**, 127204 (2012).
- [15] F. Ye *et al.*, Phys. Rev. B **85**, 180403(R) (2012).
- [16] K. Foyevtsova, H. O. Jeschke, I. I. Mazin, D. I. Khomskii, and R. Valenti, Phys. Rev. B **88**, 035107 (2013).
- [17] H.-J. Kim, J.-H. Lee and J.-H. Cho, Sci. Rep. **4**, 5253 (2014).
- [18] T. Takayama *et al.*, arXiv:1403.3296 (2014).
- [19] K. A. Modic *et al.*, Nat. Commun. **5**, 4203 (2014).
- [20] A. Biffin *et al.*, Phys. Rev. Lett. **113**, 197201 (2014).
- [21] I. Kimchi, J. G. Analytis and A. Vishwanath, Phys. Rev. B **90**, 205126 (2014).
- [22] I. Kimchi, R. Coldea and A. Vishwanath, arXiv:1408.3640v2 (2014).
- [23] E. K.-H. Lee and Y. B. Kim, arXiv:1407.4125v3 (2014).
- [24] J. Reuther, R. Thomale and S. Rachel, arXiv:1404.5818v2 (2014).
- [25] Y. Singh and P. Gegenwart, Phys. Rev. B **82**, 064412 (2010).
- [26] Y. Li *et al.*, arXiv:1410.4243 (2014).
- [27] E. Beaupaire, J. C. Merle, A. Daunois, and J. Y. Bigot, Phys. Rev. Lett. **76**, 4250 (1996).
- [28] B. Koopmans *et al.*, Nature Mater. **9**, 259 (2009).
- [29] T. Kise *et al.*, Phys. Rev. Lett. **85**, 1986 (2000).
- [30] T. Ogasawara *et al.*, Phys. Rev. Lett. **94**, 087202 (2005).
- [31] C. L. S. Kantner *et al.*, Phys. Rev. B **83**, 134432 (2011).
- [32] B. Koopmans, J. J. M. Ruigrok, F. Dalla Longa, and W. J. M. de Jonge, Phys. Rev. Lett. **95**, 267207 (2005).
- [33] Z. Alpichshev, F. Mahmood, G. Cao, and N. Gedik, Phys. Rev. Lett. **114**, 017203 (2015).